

A Three-Dimensional Ferromagnet, $[\text{Ni}(\text{dipn})_3][\text{Cr}(\text{CN})_6]_2 \cdot 3\text{H}_2\text{O}$ (dipn = dipropylene triamine), Based on a Cubic $\text{Cr}_8\text{Ni}_{12}$ Unit

Wakako Kaneko,[†] Masaaki Ohba,^{*†} Hisashi Ōkawa,[‡] and Susumu Kitagawa^{*†}

Department of Synthetic Chemistry and Biological Chemistry, Graduate School of Engineering, Kyoto University, Katsura, Nishikyo-ku, Kyoto 615-8510, Japan, and Department of Chemistry, Faculty of Science, Kyushu University, 6-10-1 Hakozaki, Higashi-ku, Fukuoka 812-8581, Japan

Received April 24, 2006

The combination of Ni^{2+} , dipropylene triamine (dipn), and $[\text{Cr}(\text{CN})_6]^{3-}$ affords the cyanide-bridged bimetallic assembly, $[\text{Ni}(\text{dipn})_3][\text{Cr}(\text{CN})_6]_2 \cdot 3\text{H}_2\text{O}$ (**1**). This compound crystallizes in cubic space group $Pa\bar{3}$, with $a = b = c = 20.9742$ (7) Å and $Z = 8$. A three-dimensional network is constructed on the basis of a $\text{Cr}_8\text{Ni}_{12}$ cubane unit formed by an alternate array of $[\text{Cr}(\text{CN})_6]^{3-}$ and $[\text{Ni}(\text{dipn})_3]^{2+}$ units through Cr–CN–Ni–NC–Cr edges. Cryomagnetic studies reveal a ferromagnetic interaction between Cr^{III} and Ni^{II} ions and a long-range ferromagnetic ordering below 42 K with very small coercive field. To the best of our knowledge, this compound is the first “complete ferromagnet” providing three-dimensional ferromagnetic interaction through a three-dimensional bridging structure that is based on a cubic unit among general metal-oxide and molecule-based magnets. Magneto-optical studies demonstrate a strong correlation between magnetic and optical properties.

Introduction

Molecule-based magnets have been developed in an interdisciplinary research area in the past two decades. On the basis of the past achievements, current interest is targeted on multifunctional magnets with other physical and/or chemical properties such as optical properties, electric conductivity, chirality, porosity, etc.^{1–9} In this field, there has been a common issue, so-called low dimensionality,

against feasible magnetic and/or electric properties as far as the use of molecules as building units. Although many efforts have been made to overcome the intrinsic low dimensionality of molecule-based magnets, three-dimensionality on the properties is still an important issue.

* To whom correspondence should be addressed. Fax: 81-75-383-2732. Telephone: 81-383-2807. E-mail: ohba@sbchem.kyoto-u.ac.jp.

[†] Kyoto University.

[‡] Kyushu University.

- (1) Kahn, O. *Molecular Magnetism*, VCH: Weinheim, Germany, 1993.
- (2) (a) Miller, J. S.; Epstein, A. J.; Reiff, W. M. *Chem. Rev.* **1988**, *88*, 201. (b) Miller, J. S.; Calabrese, J. C.; Rommelmann, H.; Chittipeddi, S. R.; Zhang, J. H.; Reiff, W. M.; Epstein, A. J. *J. Am. Chem. Soc.* **1987**, *109*, 769. (c) Miller, J. S.; Drillon, M. *Magnetism: Molecules to Materials*; Wiley–VCH: Weinheim, Germany, 2001–2003; Vol. I–IV.
- (3) (a) Verdaguer, M.; Pei, Y.; Kahn, O.; Sletten, J.; Renard, J. P. *Inorg. Chem.* **1987**, *109*, 769. (b) Kahn, O.; Pei, Y.; Verdaguer, M.; Renard, J. P.; Sletten, J. *J. Am. Chem. Soc.* **1988**, *110*, 782. (c) Verdaguer, M.; Bleuzen, A.; Marvaud, V.; Vaissermann, J.; Seuleiman, M.; Desplanches, C.; Scuille, A.; Train, C.; Garde, R.; Gelly, G.; Lomenech, C.; Rosenman, I.; Veillet, P.; Cartier, C.; Villain, F. *Coord. Chem. Rev.* **1999**, *190*, 1023. (d) Ferlay, S.; Mallah, T.; Ouahès, R.; Veillet, P.; Verdaguer, M. *Nature* **1995**, *378*, 701. (e) Kahn, O. *Nature* **1995**, *378*, 667. (f) Mallah, T.; Thiebaut, S.; Verdaguer, M.; Veillet, P. *Science* **1993**, *262*, 1554. (g) Verdaguer, M. *Science* **1996**, *272*, 698.
- (4) (a) Caneschi, A.; Gatteschi, D.; Sessoli, R.; Ray, P. *Acc. Chem. Res.* **1989**, *22*, 392. (b) Caneschi, A.; Gatteschi, D.; Malendri, M. C.; Ray, P.; Sessoli, R. *Inorg. Chem.* **1990**, *29*, 4228.
- (5) (a) Sato, O.; Iyoda, T.; Fujishima, A.; Hashimoto, K. *Science* **1996**, *272*, 49. (b) Sato, O.; Iyoda, T.; Fujishima, A.; Hashimoto, K.; *Science* **1996**, *272*, 704. (c) Gadet, V.; Mallah, T.; Castro, I.; Verdaguer, M. *J. Am. Chem. Soc.* **1992**, *114*, 9213. (d) Ently, W. R.; Girolani, G. S. *Science* **1995**, *268*, 397. (e) Gadet, V.; Mallah, T.; Castro, I.; Verdaguer, M. *J. Am. Chem. Soc.* **1992**, *114*, 9213. (f) Kahn, O. *Adv. Inorg. Chem.* **1995**, *43*, 248.
- (6) (a) Ohba, M.; Ōkawa, H. *Coord. Chem. Rev.* **2000**, *198*, 313. (b) Ōkawa, H.; Ohba, M. *Bull. Chem. Soc. Jpn.* **2002**, *75*, 1191. (c) Ohba, M.; Yamada, M.; Usuki, N.; Ōkawa, H. *Mol. Cryst. Liq. Cryst.* **2002**, *379*, 241. (d) Ohba, M.; Usuki, N.; Fukita, N.; Ōkawa, H. *Angew. Chem., Int. Ed.* **1999**, *38*, 1795. (e) Usuki, N.; Yamada, M.; Ohba, M.; Ōkawa, H. *J. Solid State Chem.* **2001**, *159*, 328. (f) Fukita, N.; Ohba, M.; Ōkawa, H.; Matsuda, K.; Iwamura, H. *Inorg. Chem.* **1998**, *37*, 842. (g) Ohba, M.; Ōkawa, H.; Fukita, N.; Hashimoto, Y. *J. Am. Chem. Soc.* **1997**, *119*, 1011.
- (7) (a) Ohkoshi, S.; Mizuno, M.; Hung, G.; Hashimoto, K. *J. Phys. Chem. B* **2000**, *104*, 9365. (b) Ohba, M.; Iwamoto, T.; Ōkawa, H. *Chem. Lett.* **2002**, 1046. (c) Ohba, M.; Iwamoto, T.; Kaneko, W.; Kitagawa, S.; Ōkawa, H. *Polyhedron* **2005**, *24*, 2839.
- (8) (a) Inoue, K.; Imai, H.; Ghalasaki, P. S.; Kikuchi, K.; Ohba, M.; Ōkawa, H.; Yakhmi, J. V. *Angew. Chem., Int. Ed.* **2001**, *40*, 4242. (b) Inoue, K.; Kikuchi, K.; Ohba, M.; Ōkawa, H. *Angew. Chem., Int. Ed.* **2003**, *42*, 4810.
- (9) (a) Coronado, E.; Galán-Mascarós, J. R.; Gómez-García, C. J.; Laukhin, V. *Nature* **2000**, *408*, 447. (b) Wang, Z.; Zhang, B.; Fujiwara, H.; Kobayashi, H.; Kurmoo, M. *Chem. Commun.* **2004**, 416. (c) Cui, H.; Takahashi, K.; Okano, Y.; Kobayashi, H.; Wang, Z.; Kobayashi, A. *Angew. Chem., Int. Ed.* **2005**, *44*, 2.

Here, we targeted a preparation of a complete ferromagnet. “Complete ferromagnet” means a magnet operating a 3-D ferromagnetic interaction through a 3-D isotropic network structure. Such magnets having 3-D structural and ferromagnetic networks are rare among general metal-oxides and molecule-based magnets, because an antiferromagnetic interaction usually operates between magnetic centers. Sophisticated molecular designs and synthetic strategies are necessary for the creation of the complete ferromagnet.

A promising strategy for producing molecular-based magnets is to create a bimetallic network by assembling two kinds of paramagnetic metal ions. Bimetallic network structures are generally constructed by the reaction between a “building block” with coordination ability and a “connecting block” providing two or more coordinatable sites to accept the donation from the building block. Hexacyano-metalate(III) ions, $[\text{M}(\text{CN})_6]^{3-}$, have widely been used as building blocks for affording Prussian-blue analogues, well-known molecule-based magnets showing high T_C , together with a simple metal ion.^{3,5} We have extensively studied the structures and magnetic properties of bimetallic compounds derived from the reaction of $[\text{M}(\text{CN})_6]^{3-}$ ($\text{M}^{\text{III}} = \text{Cr}, \text{Fe}, \text{Co}$) as a building block with $[\text{M}(\text{L})_n]^{2+}$ ($\text{M}^{\text{II}} = \text{Mn}$ ($n = 1$), Ni ($n = 2$); $\text{L} =$ diamine derivatives) as a connecting block.^{6,8} In this work, a new cyanide-bridged bimetallic assembly, $[\text{Ni}(\text{dipn})_3][\text{Cr}(\text{CN})_6]_2 \cdot 3\text{H}_2\text{O}$ (**1**; dipn = dipropylentriamine) has been prepared using $[\text{Cr}(\text{CN})_6]^{3-}$ and $[\text{Ni}(\text{dipn})_2]^{2+}$ as the building block and connecting block, respectively. The triamine coligand (dipn) gives three labile sites around the Ni ion in the connecting block, which is sterically suitable for accepting the donations from the building blocks and for constructing the multidimensional structure.^{6b,c} A 3-D isotropic network structure constructed from Cr–CN–Ni linkages should provide the ferromagnetic interaction between Cr^{III} and Ni^{II} ions because of the strict orthogonality of magnetic orbitals.¹

Experimental Section

Physical Measurements. Elemental analyses of carbon, hydrogen, and nitrogen were obtained at The Service Center of Elemental Analysis of Kyushu University. Infrared spectra were measured using a KBr disk with a Perkin–Elmer Spectrum BX FT-IR system. Magnetic susceptibilities of polycrystalline samples were measured on a Quantum Design MPMS-XL5R SQUID susceptometer in the temperature range 2–300 K with an applied field of 500 G. Samples were put into a gelatin capsule, mounted inside straw, and then fixed to the end of the sample-transport rod. Diamagnetic corrections were made with Pascal’s constants.¹⁰ Effective magnetic moments were calculated by the equation $\mu_{\text{eff}} = (8\chi_{\text{M}}T)^{1/2}$, where χ_{M} is the molar magnetic susceptibility corrected for diamagnetism of the constituting atoms. Field dependences of magnetization were measured under a field range of 0–50 kG. Magneto-optical properties were measured as Faraday ellipticity under an applied field parallel to the incident light in the temperature range 6–300 K. A circular dichroism spectrometer (JASCO J-820), equipped with an electromagnet ($H = -15$ to $+15$ kG) and a cryostat was used for magneto-optical studies. The temperature region should

Table 1. Crystallographic Parameters of $[\text{Ni}(\text{dipn})_3][\text{Cr}(\text{CN})_6]_2 \cdot 3\text{H}_2\text{O}$ (**1**)

	1
formula	$\text{C}_{30}\text{H}_{57}\text{Ni}_{21}\text{Cr}_2\text{Ni}_3$
fw	1039.99
T (K)	243
cryst syst	cubic
space group	$Pa\bar{3}$ (No. 205)
$a = b = c$ (Å)	20.9742(7)
$\alpha = \beta = \gamma$ (deg) ^a	90
V (Å ³)	9226.90(1)
Z	8
D_{calcd} (g cm ⁻³)	1.601
μ (Mo $K\alpha$) (cm ⁻¹)	17.25
no. of reflns	3507
R (all data)	0.078
R_w (all data)	0.093
$R1$ ($I > 2\sigma(I)$)	0.031
GOF	0.77

$$R = \sum(F_o^2 - F_c^2)/\sum F_o^2, R_w = [(\sum w(F_o^2 - F_c^2)^2/\sum w(F_o^2)^2)]^{1/2}, R1 = \sum||F_o| - |F_c||/\sum|F_o|.$$

correspond to that of the magnetic measurement. However, the lower limit of the cryostat for magneto-optical measurement was 6 K. To stabilize the temperature of the cryostat, we made a radiant heat shield to fit the distance of magnetic poles and set a silicone diode sensor for monitoring correct temperature at the sample position. KBr pellets were made for the actual measurement.¹¹

Synthesis. All reagents were purchased from chemical sources and used without further purification. An aqueous solution of $\text{NiCl}_2 \cdot 6\text{H}_2\text{O}$ (71 mg, 0.3 mmol) with dipn (78 mg, 0.6 mmol) and an aqueous solution of $\text{K}_3[\text{Cr}(\text{CN})_6]$ (65 mg, 0.2 mmol) were placed in each side of an H-shaped tube. The two solutions were slowly diffused over two weeks to obtain purple dodecahedral crystals of $[\text{Ni}(\text{dipn})_3][\text{Cr}(\text{CN})_6]_2 \cdot 3\text{H}_2\text{O}$ (**1**). They were separated from the yellow precipitations by decantation, collected by suction filtration, and washed with water. All the operations for the synthesis were carried out in the dark to avoid the decomposition of $[\text{Cr}(\text{CN})_6]^{3-}$. Yield: 49 mg (46%). Elemental anal. Calcd for $\text{C}_{30}\text{H}_{57}\text{N}_{21}\text{Cr}_2\text{Ni}_3\text{O}_3$: C, 34.65; H, 5.52; N, 28.28. Found: C, 35.14; H, 5.49; N, 28.44. Selected FT-IR data (ν_{CN} , cm⁻¹) using KBr disks: 2154, 2137.

X-ray Structure Determination. Crystal parameters are summarized in Table 1. All measurements were carried out at 243 K on a Rigaku/MSC Mercury CCD diffractometer with graphite-monochromated Mo $K\alpha$ radiation ($\lambda = 0.71070$ Å). The structure was solved by direct methods (SIR 92) and followed successive Fourier and difference Fourier syntheses; it was refined by full-matrix least squares on F^2 . All non-hydrogen atoms were refined anisotropically. All hydrogen atoms were added geometrically and refined using a riding model. All calculations were performed using the teXsan crystallographic software package of MSC.¹² CIF data has been deposited at the Cambridge Crystallographic Data Center (CCDC) as supplementary publication number CCDC-297338.

Results and Discussion

Preparation. $[\text{Ni}(\text{dipn})_3][\text{Cr}(\text{CN})_6]_2 \cdot 3\text{H}_2\text{O}$ (**1**) was obtained as dodecahedral crystals by the reaction of $\text{NiCl}_2 \cdot 6\text{H}_2\text{O}$, dipn, and $\text{K}_3[\text{Cr}(\text{CN})_6]$ in a 3:6:2 molar ratio in an aqueous solution by the use of an H-shaped tube. The

(10) Boudreaux, E. A.; Mulay, L. N. *Theory and Applications of Molecular Paramagnetism*; John Wiley & Sons: New York, 1976; p 491.

(11) Andrés, R.; Brissard, M.; Gruselle, M.; Train, C.; Vaissermann, J.; Malézieux, B.; Jamet, J.-P.; Verdaguier, M. *Inorg. Chem.* **2001**, *40*, 4633.

(12) *teXsan: Crystal Structure Analysis Package*; Molecular Structure Corporation: The Woodlands, TX, 1985 & 1992.

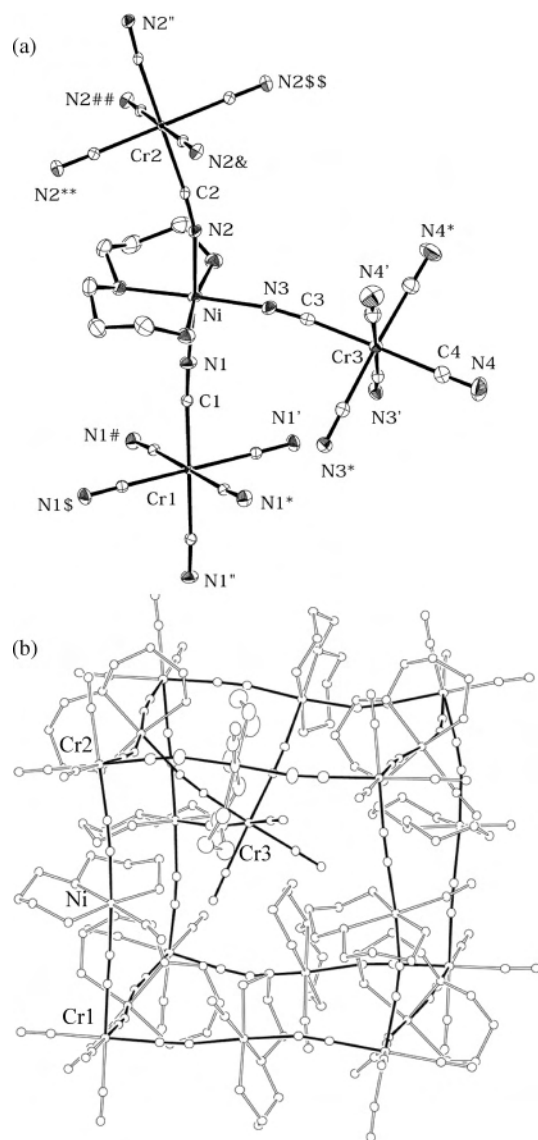


Figure 1. (a) ORTEP drawing of the asymmetric unit of [Ni(dipn)]₃[Cr(CN)₆]₂·3H₂O (**1**) with the atom numbering scheme (H₂O molecules are omitted); (b) a cubane unit of **1**.

stoichiometric reaction of the components (NiCl₂·6H₂O:dipn:K₃[Cr(CN)₆]₂·15H₂O) = 3:3:2) resulted in the immediate precipitation of Ni₃[Cr(CN)₆]₂·15H₂O. The use of excess dipn was necessary in order to avoid the precipitation of byproduct Ni₃[Cr(CN)₆]₂·15H₂O and obtain compound **1**. This compound showed two ν(C≡N) bands at 2154 and 2137 cm⁻¹, indicating the existence of bridging and terminal cyanide groups in the lattice.

Structure Description. The X-ray crystal structure analysis reveals that the asymmetric unit of [Ni(dipn)]₃[Cr(CN)₆]₂·3H₂O (**1**) consists of one [Ni(dipn)]²⁺ cation, 1/6 of a [Cr(1)(CN)₆]³⁻ anion, 1/6 of a [Cr(2)(CN)₆]³⁻ anion, 1/3 of a [Cr(3)(CN)₆]³⁻ anion and one water molecule (Figure 1). All the cyanide groups of [Cr(1)(CN)₆]³⁻ and [Cr(2)(CN)₆]³⁻ are involved in the coordination to the adjacent Ni ions. The Ni ion is in a pseudo-octahedral geometry with three amino nitrogen atoms (N5, N6, and N7) of dipn in meridional positions and three cyanide nitrogen atoms (N1, N2, and N3). In the lattice, a three-dimensional network is constructed on

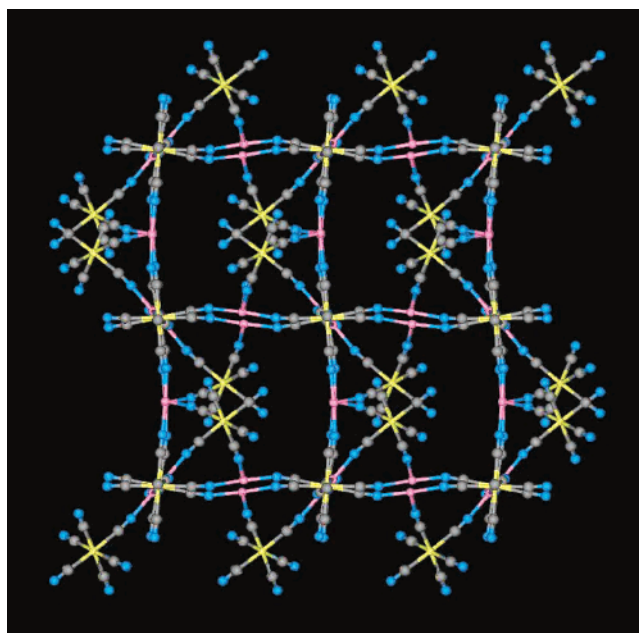


Figure 2. Three-dimensional network structure of **1**. H₂O and dipn molecules are omitted. Atoms: Ni (pink), Cr (yellow), N (blue), C (gray).

the basis of a Cr₈Ni₁₂ cubane unit formed by the array of μ₆-[Cr(1)(CN)₆]³⁻, [Ni(dipn)]²⁺, and μ₆-[Cr(2)(CN)₆]³⁻ through Cr1–CN–Ni–NC–Cr2 linkages (Figure 1). The essential framework is the same as that of [Ni(L)₂]₃[Fe^{II}(CN)₆](PF₆)₂ (L = en, tn), which we have reported previously.^{6f} In the present compound, one [Cr(3)(CN)₆]³⁻ exists inside the cubane unit, to which three adjacent [Ni(dipn)]²⁺ cations are coordinated in the facial μ₃-bridging mode, resulting in neutralization of the positive charge of the cubane unit. Three lattice water molecules are captured in the cubane unit through hydrogen-bonding to the terminal CN nitrogen atom (N4) of [Cr(3)(CN)₆]³⁻ units. The Ni–N1, Ni–N2, and Ni–N3 bond distances are 2.129(4), 2.083(3), and 2.111(4) Å, respectively (avg. 2.11 Å). The Ni–N1–C1, Ni–N2–C2, and Ni–N3–C3 bond angles are 171.8(3), 163.2(3), and 171.2(4)°, respectively (avg. 169°). The shortest Cr1···Ni, Cr2···Ni, and Cr3···Ni distances are 5.320(1), 5.227(1), and 5.313(1) Å, respectively.

In the case of another cyanide-bridged bimetallic assembly, [Ni(dipn)]₂[Ni(dipn)(H₂O)][Fe(CN)₆]₂·6H₂O (**2**) with dipn coligand, it shows a ferromagnetic ordering below T_c = 7.8 K. This compound forms a 2-D sheet structure extended by an alternate array of [Ni(1)(dipn)]²⁺ and [Fe(CN)₆]³⁻ in cis-β-μ₄-bridging mode on the bc plane, and the 2-D sheets are connected by intersheet Fe–CN–Ni linkages, with [Ni(2)-(dipn)(H₂O)]²⁺ units along the a axis providing a 3-D network structure (Figure 3).^{6g} The structure is completely different from compound **1** (see Figure 2). The difference would reflect the average of M–C–N–Ni distance in **1** and **2**. As for **1**, the estimated volume of an ideal cubane with M–CN–Ni–NC–M edges is ca. 11% larger than that of **2**. The large [Cr(CN)₆]³⁻ can provide more commodious room inside the cubane than [Fe(CN)₆]³⁻, which is one of the factors in stabilizing the sterically hindered framework.

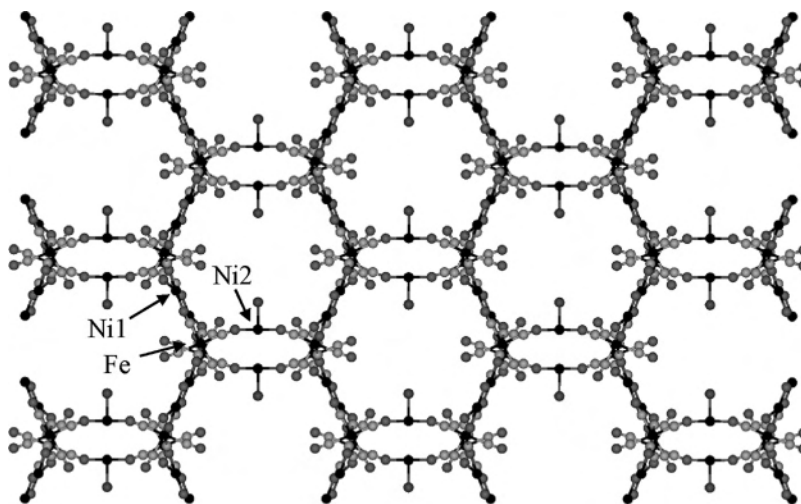


Figure 3. Projection of the 3-D network structure of $[\text{Ni}(\text{dipn})]_2[\text{Ni}(\text{dipn})(\text{H}_2\text{O})][\text{Fe}(\text{CN})_6]_2 \cdot 6\text{H}_2\text{O}$ (**2**) onto the ab plane. Lattice water and dipn molecules are omitted.

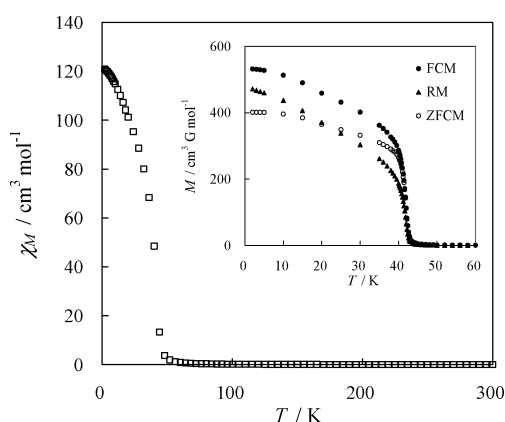


Figure 4. χ_M vs T plots of **1**. Inset: field-cooled magnetization (●), zero-field-cooled magnetization (○), and remnant magnetization (▲) for **1** under an applied field of 1 G.

Magnetic Properties. The dc magnetic susceptibility of **1** under an applied field of 500 G is shown in Figure 4 in the form of a χ_M vs T plot. The $\chi_M T$ value per $\text{Ni}^{\text{II}}_3\text{Cr}^{\text{III}}_2$ unit is $10.09 \text{ cm}^3 \text{ K mol}^{-1}$ ($8.99 \mu_B$) at room temperature, which is larger than the spin-only value ($6.750 \text{ cm}^3 \text{ K mol}^{-1}$, $7.35 \mu_B$) expected for three Ni^{II} ($S = 2/2$) and two Cr^{III} ($S = 3/2$) magnetically isolated ions with $g = 2.00$. The $\chi_M T$ value gradually increases with lowering temperature, then shows an abrupt rise below 60 K, up to a maximum value of $2560 \text{ cm}^3 \text{ K mol}^{-1}$ ($143 \mu_B$) at 32 K. Below 32 K, $\chi_M T$ decreases down to $241.4 \text{ cm}^3 \text{ K mol}^{-1}$ ($44.0 \mu_B$) at 2 K because of the saturation of magnetization. There is no minimum in the $\chi_M T$ vs T curve. The $1/\chi_M$ vs T plot (300–80 K) obeys the Curie–Weiss law with a positive Weiss constant θ of +58 K. The successive increase of χ_M and the positive θ value suggest the operation of ferromagnetic interaction between adjacent Ni^{II} and Cr^{III} ions through cyanide bridges. The ferromagnetic interaction between Ni^{II} and Cr^{III} ions can be understood by the strict orthogonality of magnetic orbitals. The rapid increase in both χ_M and $\chi_M T$ below 60 K suggests a three-dimensional long-range ferromagnetic ordering. The magnetic phase-transition temperature (T_C) is determined to be 42 K by the weak field magnetization measurement under 1 G (Figure 4 inset), the dM/dT differential plot, and the ac

magnetic susceptibility (Figures S1 and S2 of the Supporting Information). In the ac susceptibility, the in-phase signal (χ_M') shows a rapid increase below 43 K with a broad maximum and the out-of-phase signal (χ_M'') increases below 42 K under an ac magnetic field of 1 G. Because these signals were not clearly observed under an ac magnetic field of 3 G, these behaviors would be related to magnetic domain size, magnetic anisotropy, and a resulting extremely small coercive field (see next). The T_C of 42 K is about four-fifths that of the corresponding Prussian-blue analogue, $\text{Ni}_3[\text{Cr}(\text{CN})_6]_2 \cdot 15\text{H}_2\text{O}$ ($T_C = 53 \text{ K}$).^{5f} The T_C is approximately proportional to the number of the nearest magnetic centers (N) in general.^{3c} The low T_C in **1** relative to that in $\text{Ni}_3[\text{Cr}(\text{CN})_6]_2 \cdot 15\text{H}_2\text{O}$ can be explained by the number (N) of the nearest Cr centers around Ni; $N = 3$ for **1**, whereas $N = 4$ for $\text{Ni}_3[\text{Cr}(\text{CN})_6]_2 \cdot 15\text{H}_2\text{O}$ on an average. On the other hand, the T_C of the $\text{Ni}^{\text{II}}\text{-Fe}^{\text{III}}$ ferromagnet **2** (7.8 K) is very low, despite the 3-D network structure. The low T_C of **2** is associated with the lowered symmetry (C_{2v}) of the $[\text{Fe}(\text{CN})_6]^{3-}$ unit in the lattice. That is, $[\text{Fe}(\text{CN})_6]^{3-}$ under this symmetry has one unpaired electron on one of the split $d\pi$ character orbitals ($a_2(d_{xy})$, $b_1(d_{yz})$, or $b_2(d_{yz})$), so that a magnetic ordering occurs on the basis of a two-dimensional magnetic interaction through a CN bridge and weak intersheet interaction.^{6e} Similar 3-D $\text{Ni}^{\text{II}}\text{-Fe}^{\text{III}}$ cyanide-bridged magnets of low T_C (8–10 K) have been also reported.¹³ In the case of **1**, $[\text{Cr}(\text{CN})_6]^{3-}$ has three unpaired electrons on all the $d\pi$ character orbitals, $(d_{xy})^1\text{-}(d_{xz})^1(d_{yz})^1$, even under C_{2v} symmetry, which is convenient for the three-dimensional magnetic interaction and procures a higher T_C . Also, a well-structurally characterized ferromagnet, $[\text{Cu}(\text{EtOH})_2][\text{Cu}(\text{en})_2][\text{Cr}(\text{CN})_6]_2$, has been reported already.¹⁴ This compound forms a 3-D network based on gridlike layers with $N = 4$ and shows a ferromagnetic ordering at 57 K (its magnetic properties have not been fully characterized because of very low yield). The isotropic

(13) (a) Fallah, M. S. E.; Rentschler, R.; Caneschi, A.; Sessoli, R.; Gatteschi, D. *Angew. Chem., Int. Ed.* **1996**, *35*, 1947. (b) Zhang, S. W.; Fu, D. G.; Sun, W. Y.; Hu, Z.; Yu, K. B.; Tang, W. X. *Inorg. Chem.* **2000**, *39*, 1142.

(14) (a) Kou, H.-Z.; Gao, S.; Zhang, J.; Wen, G.-H.; Su, G.; Zheng, R. K.; Zhang, X. X. *J. Am. Chem. Soc.* **2001**, *123*, 11809.

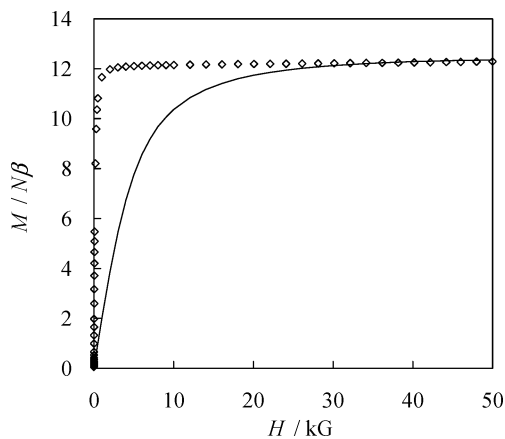


Figure 5. M vs H plot for **1** at 2 K. Solid line expresses Brillouin function for $S = 12/2$ and $g = 2.07$.

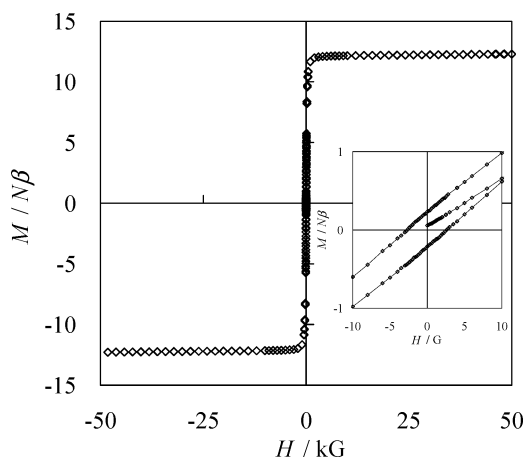


Figure 6. Magnetic hysteresis loop for **1** at 2 K. The inset is an expansion in the range of -10 to $+10$ G.

electronic configuration of $[\text{Cr}(\text{CN})_6]^{3-}$ works well for magnetic ordering in this compound; however, the T_C is lower than that of the corresponding Prussian-blue analogue, $\text{Cu}_3[\text{Cr}(\text{CN})_6]_2 \cdot 15\text{H}_2\text{O}$ ($T_C = 66$ K), despite the same N value of 4. It would not strictly form a complete ferromagnetic network as we defined, because the Cu^{II} ion in $[\text{Cu}(\text{en})]^{2+}$ is under a quasi-square-pyramidal environment with disordered arrangements of the en coligand.

The M vs H curve of **1** at 2 K shows a rapid increase to saturate above 2 kG (Figure 5). The saturation magnetization value per $\text{Ni}^{\text{II}}_3\text{Cr}^{\text{III}}_2$ unit at 50 kG is $12.35 N\beta$, which corresponds to the value of $S = 12/2$ expected for three Ni^{II} and two Cr^{III} ferromagnetically coupled ions with an average g value of 2.07. The theoretical curve based on the Brillouin function for $S = 12/2$ with $g = 2.07$ is shown as the solid line in Figure 5. The shape of the M vs H curve strongly supports the ferromagnetic ordering of **1** in the bulk.

The magnetic hysteresis loop at 2 K is given in Figure 6. The remnant magnetization ($0.25 N\beta$) is very small, and the coercive field is smaller than 3 G. The hysteresis curve is typical of soft magnets. The very small coercive field must be associated with the isotropic electronic configuration of the Cr^{III} ion and the nearly isotropic three-dimensional network structure (isotropic magnetic domain).

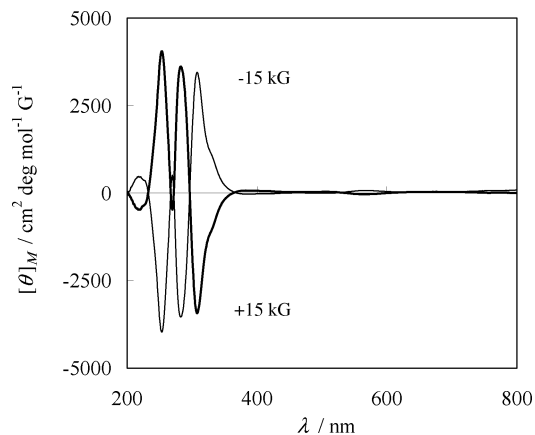


Figure 7. MCD spectra for **1** measured at 6 K under ± 15 kG.

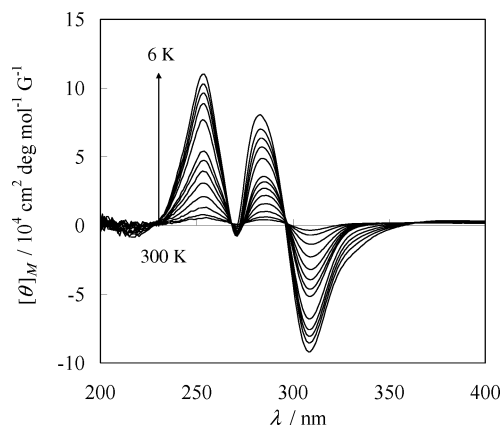


Figure 8. Temperature dependence of MCD spectra for **1** under an applied field of 200 G.

Magneto-optical Properties. The magneto-optical properties (magnetic circular dichroism, MCD) of **1** were examined by the measurement of Faraday ellipticity θ . To express magneto-optical properties, here we adopt magnetomolar ellipticity ($[\theta]_M$), which is expressed by the equation

$$[\theta]_M = \frac{\theta M}{WH} \quad (1)$$

where M is the molecular weight and W is a sample weight.¹⁵ For the actual measurement, we used a pressed KBr disk (thickness is ca. 0.1 mm) that included 1% (w/w) of the sample. The external pressure of 8 kbar for preparing the KBr disk gave no remarkable change to the magnetic behavior, which was also confirmed by magnetic measurement under an isostatic pressure to 15 kbar.

The MCD spectra of **1** measured at 6 K under the applied field of ± 15 kG are shown in Figure 7. Three dominant bands were observed around 254, 283, and 308 nm. The reflectance spectrum of **1** at room temperature is given in Figure S3 of the Supporting Information. Although it is difficult to ascribe these bands in detail because two types of $[\text{Cr}(\text{CN})_6]^{3-}$ with different symmetries (quasi- O_h and C_3)

(15) (a) Stephens, P. J. *Annu. Rev. Phys. Chem.* **1974**, *25*, 201. (b) Buckingham, A. D.; Stephens, P. J. *Annu. Rev. Phys. Chem.* **1966**, *17*, 399. (c) Schats, P. N. Q. *Rev. Phys. Chem.* **1969**, *23*, 552. (d) Schats, P. N.; McCaffery, A. J.; Suetaka, W.; Henning, G. N.; Ritchie, A. B.; Stephens, P. J. *J. Chem. Phys.* **1966**, *45*, 722.

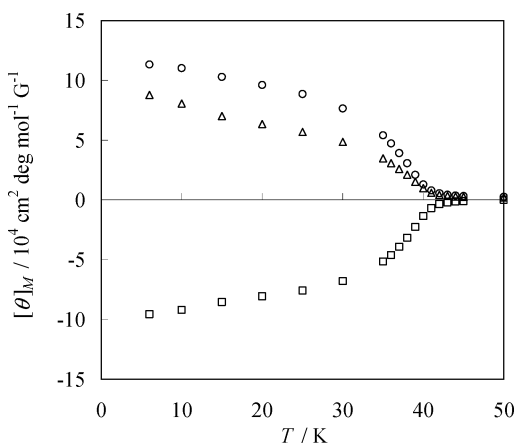


Figure 9. $[\theta]_M$ vs T plots at 254 (○), 283 (△), and 308 nm (□) under an applied field of 200 G.

exist in the crystal structure, they would be associated with a $d-d$ transition of $t_{2g} \rightarrow e_g$ and the allowed transition of $t_{2u}(\sigma) \rightarrow t_{2g}$, which is experimentally and theoretically attributed by the spectrum of the $[\text{Cr}(\text{CN})_6]^{3-}$ ion.¹⁶ In the case of paramagnetic $\text{K}_3[\text{Cr}(\text{CN})_6]$, it gives simple spectra at 6 K (Figure S4 of the Supporting Information), and signals below 300 nm are not observed well because of weak intensity. The Faraday spectrum was inverted in sign by applying a reversal magnetic field, which means all bands originate from MCD. The temperature dependences of the molar Faraday ellipticity $[\theta]_M$ in the ranges 6–300 K and 200–600 nm were measured under an applied field of 200 G (Figure 8). With decreasing temperature, the $[\theta]_M$ value was enhanced with a small shift in the peak position. The shapes of $[\theta]_M$ vs T plots at 254, 283, and 308 nm have marked resemblances to that of the χ_M vs T curve (Figures 4 and 9). This enhancement of $[\theta]_M$ reflects an increase in the internal magnetic field due to the ferromagnetic ordering. The field dependence of the MCD spectra at 254, 283, and 308 nm at 6 K also shows a small hysteresis loop similar to the magnetic hysteresis loop (Figure 10). These results demonstrate a correlation between magnetic and optical characteristics of molecule-based magnets as “colored transparent magnets”.

(16) (a) Wasielewska, E. *Inorg. Chim. Acta* **1986**, *122*, L1. (b) Hendrickx, M. F. A.; Mironov, V. S.; Chibotaru, L. F.; Ceulemans, A. *J. Am. Chem. Soc.* **2003**, *125*, 3694.

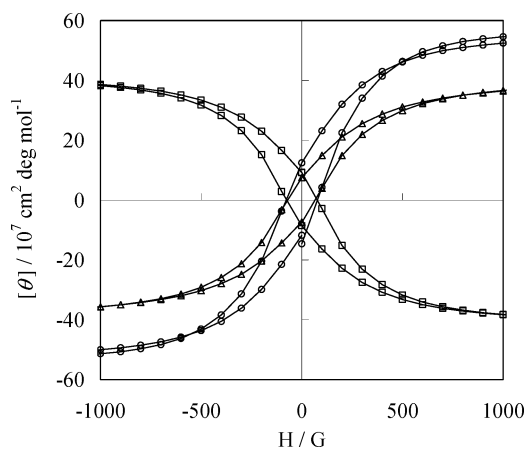


Figure 10. MCD hysteresis loops for **1** measured at 6 K and 254 (○), 283 (△), and 308 nm (□) nm.

Conclusion

In this work, a bimetallic ferromagnet, $[\text{Ni}(\text{dipn})_3][\text{Cr}(\text{CN})_6]_2 \cdot 3\text{H}_2\text{O}$ (**1**), with a 3-D isotropic network structure based on a $\text{Cr}_8\text{Ni}_{12}$ cubane unit was prepared. Compound **1** showed a long-range ferromagnetic ordering below $T_C = 42$ K with an extremely small coercive field. The isotropic electron configuration of the Cr^{III} ion under O_h symmetry and isotropic 3-D Cr–CN–Ni linkages with strict orthogonality of magnetic orbitals realized the complete 3-D ferromagnetic framework based on a cubane unit. To the best of our knowledge, this is the first example of the structurally determined complete ferromagnet. The magneto-optical studies revealed that MCD intensities attributed to LMCT bands of Cr–CN were markedly enhanced below T_C , in harmony with the long-range ferromagnetic ordering.

Acknowledgment. This work was supported by a Grant-In-Aid for Science Research in a Priority Area “Chemistry of Coordination Space” (16074209) from the Ministry of Education, Science, Sports and Culture of Japan, and Core Research for Evolutional Science and Technology (CREST), Japan Science and Technology Corporation (JST), Japan. W.K. is grateful to JSPS Research Fellowships for Young Scientists.

Supporting Information Available: Crystallographic data for compound **1** in CIF format and additional plots of data in PDF format. This material is available free of charge via the Internet at <http://pubs.acs.org>.

IC0606882